

## Optimization of the Patterning Processing and Electrical Characteristics of a Photopatternable Organosiloxane-Based Gate Dielectric for Organic Thin-Film Transistors\*

Sunho JEONG, Seong Hui LEE, Dongjo KIM and Jooho MOON\*

Department of Materials Science and Engineering, Yonsei University, Seoul 120-749

(Received 27 June 2008)

A ultraviolet (UV)-crosslinkable organosiloxane-based organic-inorganic hybrid gate dielectric for use in organic thin-film transistors was fabricated. The hybrid dielectric was synthesized via a sol-gel reaction using a mixture of a Si-based alkoxide, which contained a UV-crosslinkable organic functional group for photopatternability and a Zr-based alkoxide, which provided for a high dielectric constant ( $\sim 5.5$ ). To obtain a precisely patterned dielectric layer with a linewidth of  $3 \mu\text{m}$ , the pre-bake temperature and the UV irradiation time were optimized by investigating the evolution of the chemical structure and analyzing the photopolymerization kinetics of the UV-crosslinkable organic group. In addition, chemical groups that caused current leakage were eliminated by controlling the post-bake temperature, resulting in a gate dielectric with a dielectric strength of  $1.2 \text{ MV/cm}$ .

PACS numbers: 82.35.+t, 72.80.Sk, 81.20.Fw, 85.30.Tv

Keywords: Organic thin-film transistors, Sol-gel, Photo-patternable, Gate dielectric

### I. INTRODUCTION

Organic thin-film transistors (OTFTs) have received considerable attention recently because of their flexibility, light weight, low cost and processability. OTFTs have been considered as candidates for a wide variety of applications [1–5]. The performance of OTFTs has improved significantly in the past decade and has already reached a level comparable to that of hydrogenated amorphous-silicon transistors [6,7]. However, despite the impressive advances that have been made towards the overall improvement of OTFTs, there have been relatively few reports on patterned gate dielectrics.

Gate dielectrics are patterned for access to either the gate electrode in a bottom-gate configuration or the source/drain electrode in a top-gate configuration, in order to be applicable for active-matrix displays and integrated circuits. Photolithography, which involves patterning a photoresist, gate dielectric etching and photoresist removal, has been generally employed to pattern gate dielectrics. However, this process is rather complicated and relatively expensive. Photopatternable gate dielectrics are viable alternative materials that can simplify the complicated processing procedures and thereby reduce the manufacturing costs for modern organic electronics. The research on photoimageable gate dielectrics has been restricted to a few materials, such

as polyvinylphenol, polyimide, acryl-based polymers and sol-gel derived siloxane-based hybrid polymers [8–17]. In particular, the sol-gel derived hybrid materials can be tailored at the molecular level by controlling the chemical structure of the precursors used for the formulation. Sol-gel derived siloxane-based hybrid materials are composed of an inorganic siloxane network, a dielectric constant control unit and a photocurable organic unit. Organic components, such as unsaturated hydrocarbons or epoxide substitutes present in the glass matrix can polymerize upon illumination by UV light [18], causing decreased solubility of the irradiated parts and enabling the formation of patterns by a simple development process. A transition metal oxide is incorporated to increase the dielectric constant of the resulting hybrid material.

In a recent study, we introduced a photopatternable organosiloxane-based hybrid dielectric synthesized by a sol-gel reaction and we demonstrated that our hybrid dielectric is suitable for gate dielectrics for OTFTs [17]. In this report, we discuss the optimization of the process conditions that determine the quality of the patterned structure and the electrical characteristics of the hybrid dielectric.

### II. EXPERIMENT

Photopatternable organic-inorganic hybrid precursor solutions were prepared using a combination of 3-methacryloxypropyltrimethoxysilane (MEMO) and zir-

\*E-mail: jmoon@yonsei.ac.kr;  
Tel: +82-2-2123-2855; Fax: +82-2-365-5882

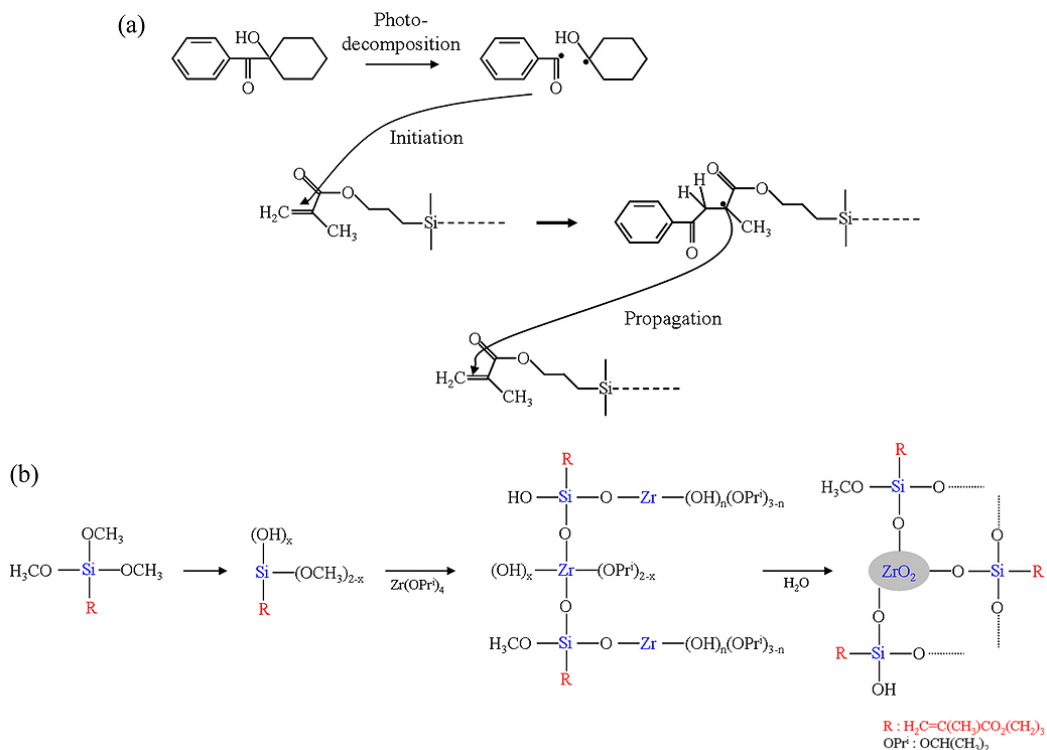


Fig. 1. (a) Schematic diagram showing the mechanism of photopolymerization initiated by interaction between photodecomposed initiator and a methacryl group (functional group of the hybrid precursor). (b) Schematic diagram showing the mechanism of formation of ZrO<sub>2</sub> particulate phase in a siloxane-based matrix.

conium isopropoxide ( $\text{Zr}(\text{OPr}^i)_4$ ). MEMO was pre-hydrolyzed with acid-catalyzed water. A mixture of  $\text{Zr}(\text{OPr}^i)_4$  and methacrylic acid in 1-propanol was combined with the prehydrolyzed MEMO solution in a molar ratio of 8 : 2 (MEMO:Zr( $\text{OPr}^i$ )). Next, deionized water was added for hydrolysis and condensation reactions between the two precursors; 1-hydroxycyclohexylphenylketone was used as the photoinitiator. After aging for an appropriate duration, the synthesized sol was filtered through a 0.2- $\mu\text{m}$  membrane filter (PTFE, Advantec MFS). All reactions were performed under nitrogen atmosphere at 25 °C in a water bath (Isotemp 3013, Fisher Scientific).

Heavily doped silicon was used as the substrate and was cleaned by a wet method using trichloroethylene, acetone, isopropyl alcohol, methyl alcohol and deionized water. Native oxide (a few angstroms thick) on the surface of the Si substrate was not removed because its presence did not cause a variation in the electrical properties of the hybrid dielectric. The sol was then spin-coated on the Si substrate and pre-baked at different temperatures to investigate the influence of the pre-bake temperature on the structural evolution of the hybrid film. Next, the film was selectively irradiated using a UV lamp (Hg-lamp, 350 W,  $\lambda < 400$  nm, Midas-System MD2-4000) with an intensity of 15 mW for a period between 0 to 30 min to determine the optimized dosage of UV irradiation for obtaining a well-patterned structure. The selectively

irradiated hybrid film was then developed in isopropyl alcohol and subsequently post-baked at either 130 °C or 170 °C. The chemical structure of the hybrid film and the microstructures of the patterned hybrid dielectric were observed by attenuated total reflectance Fourier transform infrared spectrometry (ATR-FT-IR, Jasco) and optical microscopy (Leica DMLM), respectively.

To demonstrate the influence of the structural evolution caused by the post-bake process on the electrical characteristics of the hybrid film, the electrical properties were investigated by current-voltage (I-V) measurements and capacitance-voltage (C-V) measurements at a frequency of 1 MHz using a Au/dielectric/heavily doped silicon structure. All I-V and C-V measurements were performed in air using an Agilent 5263A source-measure unit and an Agilent 4284A precision LCR meter, respectively. All samples were dehydrated in a vacuum atmosphere prior to taking the measurements.

### III. RESULTS AND DISCUSSION

A photopatternable organic-inorganic hybrid precursor solution was synthesized using a mixture of MEMO and  $\text{Zr}(\text{OPr}^i)_4$ . MEMO is a silicon-based alkoxide with three alkoxy groups and one methacryl group, which can be cross-linked by either UV light or thermal energy.

Upon UV illumination, free-radical polymerization of the methacryl group is initiated and accelerated by photodecomposed initiator, as shown in Figure 1. UV irradiation decomposes the photoinitiator into free radicals and these radicals can attack the unsaturated C=C bond in a methacryl group. Cross-links between methacryl groups are created via transformation of C=C bonds into C-C bonds, endowing a negative-resist photopatternable character.

$Zr(OPr^i)_4$  is a typical zirconium-based alkoxide with four alkoxy groups and it was incorporated to increase the dielectric constant of the hybrid dielectric film. As reported previously [17], isolated crystalline- $ZrO_2$  clusters are dispersed in the amorphous silicon dioxide matrix and their crystal sizes are around 10 nm. The mechanism of formation of this transition metal oxide particulate phase is depicted in Figure 1b. Firstly, MEMO is partially hydrolyzed in a prehydrolysis step. Then, during the injection step of  $Zr(OPr^i)_4$ , the Si-OH groups join with the Zr precursor via hydrolysis-condensation, producing -Si-O-Zr- networks as an intermediate product. Subsequently, rehydrolysis and polycondensation of -Si-O-Zr- upon the introduction of additional water result in the growth of  $ZrO_2$  particles nucleated within the siloxane-based matrix. Because the  $ZrO_2$  nuclei are surrounded by a rigidly grafted siloxane backbone, their growth is limited to a few nanometers. These dispersed  $ZrO_2$  inclusions, or clusters, effectively increase the dielectric constant of the hybrid dielectric above 5.5, whereas the dielectric constant of pure siloxane-based materials are  $\sim 3.9$ .

In order to pattern the as-prepared hybrid film, successive procedures such as pre-baking, UV irradiation and post-baking are necessary. Pre-baking is required to evaporate the solvents in the spin-coated film and to improve adhesion of the film onto substrate, without inducing any chemical reaction between the synthesized hybrid precursor monomeric species. At pre-bake temperatures below 90 °C, solvents in the film were not completely removed, causing the film to adhere to the overlying photomask and thus hindering the photolithographic patterning process. Pre-baking at temperatures above 90 °C allowed the hybrid films to completely dry, forming a non-sticky and solid surface. However, pre-baking at 110 °C prevented the unexposed portions of the hybrid films from being dissolved by the developing solvent, regardless of the amount of UV irradiation. This effect is a result of a thermally-driven chemical reaction that increased the connectivity between the hybrid precursor monomeric species. To investigate the evolution of the chemical structure of the hybrid film around 110 °C, ATR-FT-IR spectra of pre-baked hybrid films were analyzed as shown in Figure 2. Absorption bands at  $1720\text{ cm}^{-1}$  and  $1643\text{ cm}^{-1}$  result from the C=O stretching mode and the C=C stretching mode, respectively, of methacryl groups [19]. Absorption bands at  $1168\text{ cm}^{-1}$ ,  $1120\text{ cm}^{-1}$  and  $945\text{ cm}^{-1}$  are assigned to the -CH<sub>3</sub> rocking mode of Si-OCH<sub>3</sub>, the Si-O-Si asymmetric stretching

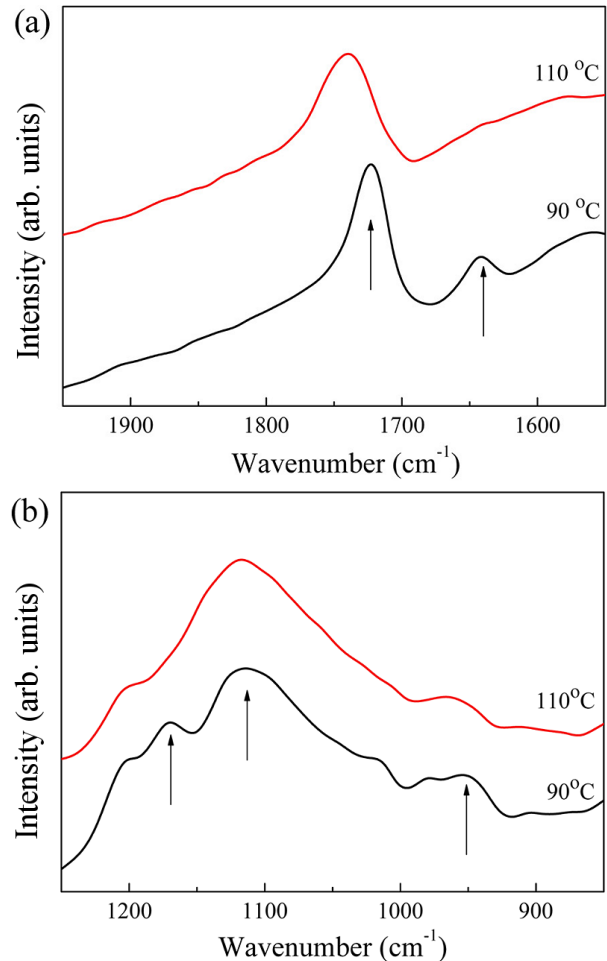


Fig. 2. ATR-FT-IR absorption spectra of (a) methacryl and (b) silanol, methoxy and silicate groups in films pre-baked at 90 and 110 °C. (Film thickness = 265 nm).

mode and the Si-OH asymmetric stretching mode, respectively [20]. While peaks due to the C=C bonds of the methacryl groups, the Si-OCH<sub>3</sub> groups and the Si-OH groups are present for hybrid films pre-baked at 90 °C, peaks resulting from the C=C bonds of the methacryl groups and the Si-OCH<sub>3</sub> groups completely disappear and the peak resulting from the Si-OH groups diminishes for hybrid films pre-baked at 110 °C. This indicates that at 110 °C polymerization of the unsaturated C=C bonds goes to completion and the condensation reaction that consumes the alkoxy and silanol groups proceeds to some extent. Therefore, pre-baking at 90 °C is adequate to evaporate the solvents without initiating the sol-gel chemical reaction and thermally inducing polymerization of the methacryl groups.

The UV-irradiation procedure plays a dominant role in patterning a photopatternable hybrid dielectric material. Figure 3 shows the ATR-FT-IR absorption spectra of hybrid films illuminated using different exposure times. We observed that peaks due to the C=C bonds diminished with increasing irradiation times, indicating that

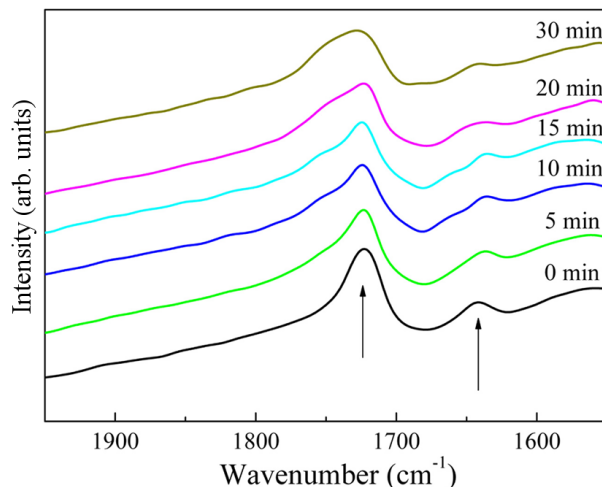


Fig. 3. ATR-FT-IR absorption spectra of methacryl in films irradiated from 0 to 30 min. All samples were pre-baked at 90 °C prior to UV irradiation. (Film thickness = 265 nm).

UV irradiation induces the cross-linking of the methacryl groups. However, the UV irradiation for a long time increases the resistance against a developing solvent when the pattern formed, but also deteriorates the pattern quality, as shown in Figure 4. The kinetics of the photopolymerization of the methacryl groups is related to the radicals induced by the UV-decomposed initiator. Since the formation and destruction of radicals both occur rapidly after the onset of the reaction, we can assume that the free radical-induced polymerization is a steady state process. The steady-state polymerization kinetics can be expressed by the following equation [21]:

$$-\frac{d[M]}{dt} = k_p[M] \sqrt{\frac{fk_d[I]}{k_t}},$$

where  $[M]$  is the total concentration of all chain radicals,  $[I]$  is the concentration of the initiator and  $f$  is the fraction of initiator radicals that are actually involved in the polymerization and are not consumed by side reactions.  $k_p$ ,  $k_t$  and  $k_d$  represent the rate constants for propagation, termination and dissociation of the initiator, respectively. Since  $[I]$ ,  $k_t$ ,  $k_d$  and  $f$  are independent of  $[M]$ , a linear relationship should be found between the  $\ln [M]$  and reaction time (*i.e.* UV irradiation time).  $[M]$  can be represented by the area of the band due to the C=C stretching mode at  $1643 \text{ cm}^{-1}$ , because the band area is proportional to the methacryl monomer concentration. As shown in Figure 5, the dependency of the  $\ln [M]$  on the UV irradiation time can be divided into three stages and each stage is characterized by a linear behavior of distinct slopes. This means that each different stage of the polymerization conforms to general free-radical polymerization kinetics. The band area abruptly reduced during the initial UV illumination (stage I), followed by a gradual decrease in the band area after 3 min of UV illumination (stage II). In stage I, the C=C bonds

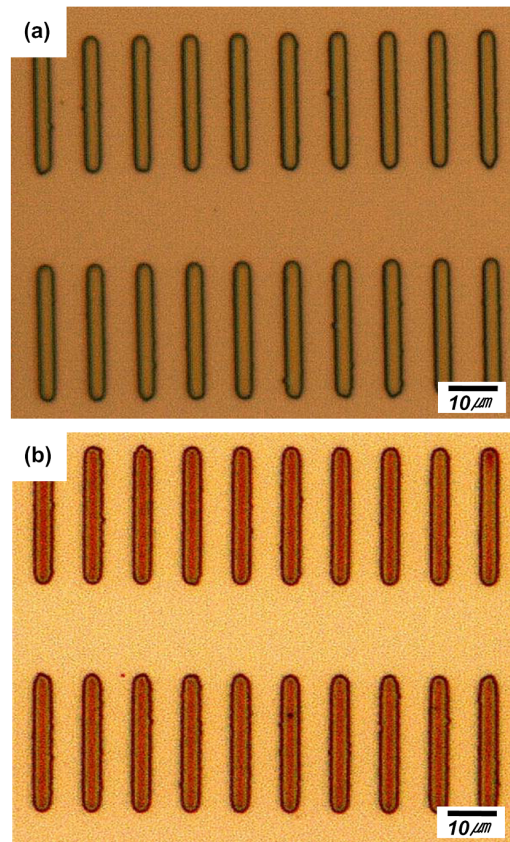


Fig. 4. Optical microscopy image of patterned hybrid dielectric film after UV irradiation for (a) 15 min and (b) 30 min. The linewidths of the patterned hybrid film irradiated for 15 min and 30 min are 3  $\mu\text{m}$  and 3.5  $\mu\text{m}$ , respectively. The linewidth of the pattern on the photomask was 3  $\mu\text{m}$ .

are rapidly consumed by vigorous initiation of the polymerization of the methacryl groups, which starts with the photodecomposition of the photoinitiator. In stage II, the consumption of the C=C bonds slow down since the propagation step is restricted by a sluggish diffusion of the monomeric species in the solid phase. However, after 15 min of UV illumination (stage III), a rapid polymerization reaction starts again. Too much UV irradiation provides excess energy for photodecomposed initiator to migrate into regions shadowed by the photomask, resulting in cross-linking of methacryl groups in undesired areas. This is why the patterned structure illuminated for 30 min exhibits a broader linewidth and irregular shape at the edge of patterns (Figure 4(b)).

Post-baking also plays an important role in fabricating a gate dielectric of high quality. Even after UV irradiation, the unsaturated C=C bonds, methoxy groups and silanol groups can remain, which deteriorates the electrical properties of the hybrid film; thus, these groups need to be completely eliminated by cross-linking the unsaturated C=C bonds and inducing the condensation reaction via post-baking. As shown in Figure 6, the C=C bonds, methoxy groups and silanol groups were removed

Table 1. Electrical characteristics of hybrid films prepared without post-baking and by post-baking at 170 °C. All samples were pre-baked at 90 °C and irradiated by UV for 15 min prior to post-baking. The film thickness of all the hybrid films is 265 nm.

Hybrid Dielectric Film	Dielectric Strength <sup>#</sup> (MV/cm)	Capacitance (nF/cm <sup>2</sup> )	Dielectric Constant
Without post-baking	0.2	24.8	7.5
Post-baked at 170 °C	1.2	18.2	5.5

<sup>#</sup> Defined as the electric field at a current density of 10<sup>-6</sup> A/cm<sup>2</sup>.

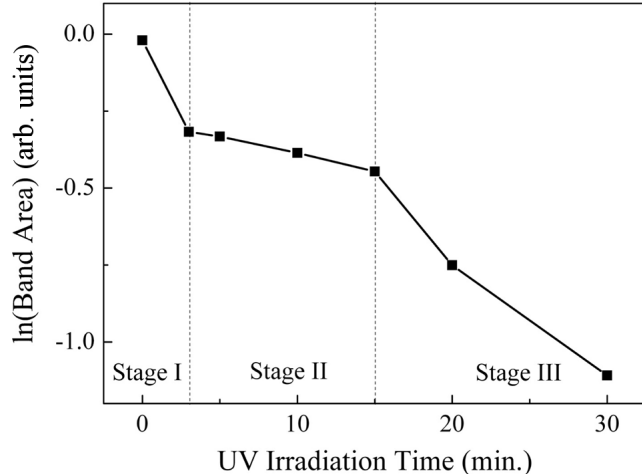


Fig. 5. Logarithmic plot of the area of the C=C stretching mode (1643 cm<sup>-1</sup>) as a function of UV illumination time.

by post-baking at temperatures above 130 °C. However, post-baking at around 170 °C is required to evaporate adsorbed water and residual organic solvent. During deposition of electrodes or semiconductor materials that are placed onto the hybrid dielectric film for the fabrication of OTFTs, vapors of any remaining water and other solvents can damage the overlying electroactive materials. To confirm the improvement of electrical properties by post-baking, I-V and C-V measurements were obtained for hybrid films post-baked at 170 °C and for films prepared without post-baking; the results are shown in Figure 7 and Table 1. Hybrid films prepared without post-baking exhibited higher dielectric constants and extremely inferior current leakage, compared to post-baked hybrid film. A dielectric strength of 1.2 MV/cm, measured for the post-baked hybrid film, is sufficient for gate dielectric applications for OTFTs and there is no serious current leakage problem [17]. We believe that residual C=C bonds, methoxy groups and silanol groups can increase the dielectric constant of the hybrid film, as they act as permanent dipoles. The effect of these groups can be viewed as a benefit since the threshold voltage of the transistor would be lowered; however, at the same time, these groups can considerably deteriorate the current leakage behavior. We have recently reported that silanol groups in sol-gel derived dielectrics play a role

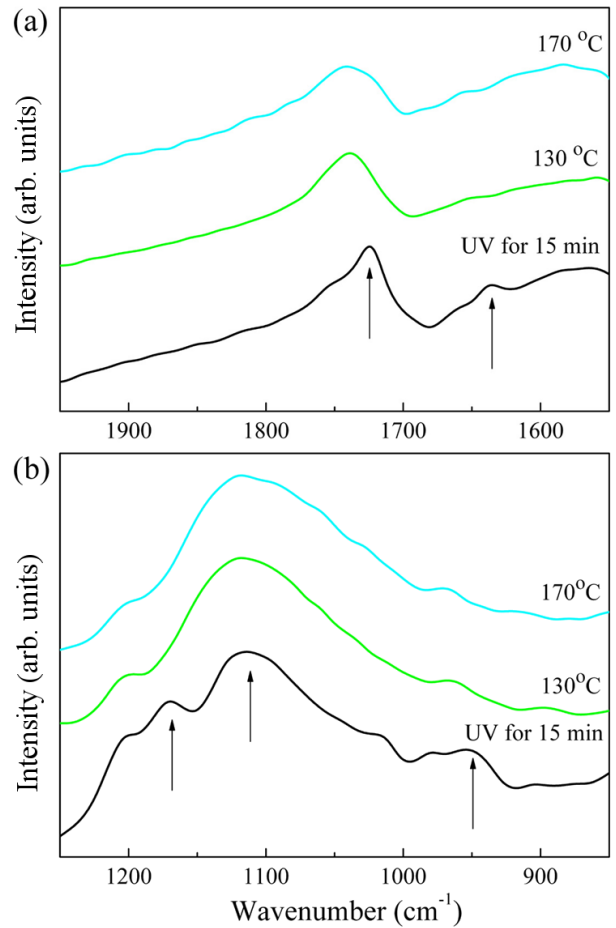


Fig. 6. ATR-FT-IR absorption spectra of (a) methacryl and (b) silanol, methoxy and silicate groups in films prepared without post-baking and post-baked at 130 °C and 170 °C. All samples were pre-baked at 90 °C and irradiated by UV for 15 min prior to post-baking. (Film thickness = 265 nm).

as a trap source of Poole-Frenkel conduction [22]. Both the C=C bonds and the methoxy groups are electronically polarizable, so that they can act as trap sources for electrons. Therefore, a post-baking treatment that can remove all functional chemical groups having electronic polarizabilities is essential for obtaining a hybrid dielectric film for OTFTs.

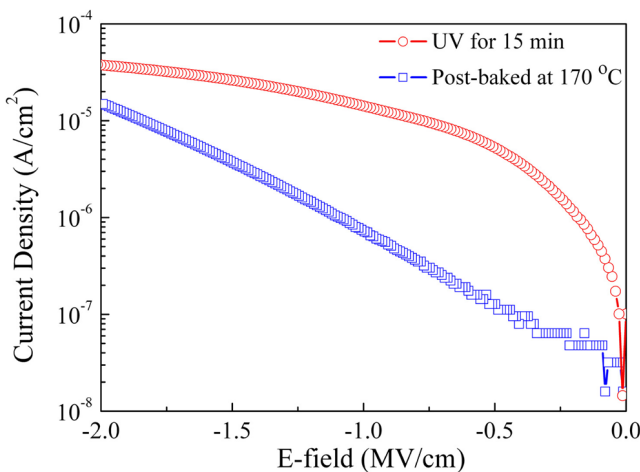


Fig. 7. Current leakage behavior of hybrid dielectric films prepared without post-baking and films post-baked at 170 °C. All samples were pre-baked at 90 °C and irradiated by UV for 15 min prior to post-baking. (Film thickness = 265 nm).

#### IV. CONCLUSION

We have synthesized an organosiloxane-based photopatternable dielectric material for OTFTs. The hybrid material is composed of a siloxane-based matrix, including both  $ZrO_2$  nanoclusters for a high dielectric constant and methacryl groups for negative-resist photopatternability. By investigating the chemical structure of the hybrid film during the pre-baking process, we determined the optimal pre-baking temperature at which the dielectric film can be dried without causing a thermally-induced chemical reaction of the monomeric species. The UV irradiation time was also optimized for obtaining a well-patterned structure with a linewidth of 3  $\mu$ m, based on an understanding of the polymerization kinetics of methacryl groups. The influence of the post-baking process on the electrical properties of the hybrid dielectric film was further investigated and a post-baking temperature of 170 °C produced a hybrid dielectric material with low current leakage that can be used for high performance OTFTs.

#### ACKNOWLEDGMENTS

This work was supported by the Korea Science and Engineering Foundation (KOSEF) through the National Research Lab Program funded by the Ministry of Science and Technology (No. R0A-2005-000-10011-0). Partial support was also provided by Samsung Electronics Co. Ltd. and the Second Stage of the Brain Korea 21 Project in 2007.

#### REFERENCES

- C. D. Dimitrakopoulos and D. J. Mascaro, IBM J. Res. Dev. **45**, 11 (2001).
- H. Edzer, A. Huitema, G. H. Gelinck, J. Bas, P. H. Van der Putten, K. E. Kuijk, K. M. Hart, E. Cantatore and D. M. De Leeuw, Adv. Mater. **14**, 1201 (2002).
- B. K. Crone, A. Dodabalapur, Y. Y. Lin, R. W. Filas, A. Bao, A. Laduca, R. Sarpeshkar, H. E. Katz and W. Li, Nature **403**, 521 (2000).
- B. K. Crone, A. Dodabalapur, R. Sarpeshkar, A. Gelperin, H. E. Katz and Z. N. Bao, J. Appl. Phys. **91**, 10140 (2002).
- Y. H. Kim, J. I. Han and D. G. Moon, J. Korean Phys. Soc. **48**, S118 (2006).
- J. H. Lee, K. S. Shin, J. H. Park and M. K. Han, J. Korean Phys. Soc. **48**, S76 (2006).
- S. F. Nelson, Y. Y. Lin, D. J. Gundlach and T. N. Jackson, Appl. Phys. Lett. **72**, 1854 (1998).
- S. H. Lee, D. J. Choo, S. H. Han, J. H. Kim, Y. R. Son and J. Jang, Appl. Phys. Lett. **90**, 033502 (2007).
- U. Hass, A. Hasse, V. Satzinger, H. Pichler, G. Leising, G. Jakopic, R. Houbertz, G. Domann, A. Schmitt and B. Stadlober, Phys. Rev. B **73**, 235339 (2006).
- G. H. Kim, S.-M. Yoon, C. A. Kim, K.-H. Baek, I.-K. You, S. Y. Kang, S. D. Ahn and K. S. Suh, J. Korean Phys. Soc. **49**, 1239 (2006).
- G. H. Gelinck, H. E. A. Huitema, E. V. Veenendaal, E. Cantatore, L. Schrijemakers, J. B. P. H. V. Derputten, T. C. T. Genus, M. Beenhakkers, J. B. Giesbers, B. H. Huisman, E. J. Meijer, E. Mena, E. J. Touwslager, A. W. Marsman, B. J. E. V. Rens and D. M. D. Leeuw, Nat. Mater. **3**, 106 (2004).
- Y. M. Kim, S. W. Pyo, J. S. Kim, J. H. Shim, C. H. Sun and Y. K. Kim, Opt. Mater. **21**, 425 (2002).
- J. H. Lee, S. H. Kim, G. H. Kim, J.-I. Lee, Y. S. Yang, H. Y. Chu, J. Oh, L.-M. Do, T. Zyung and J. Jang, J. Korean Phys. Soc. **42**, 614 (2003).
- S. J. Choi, S. Lee, K. K. Han, K. Lee, D. Kim, J. Kim and H. H. Lee, Appl. Phys. Lett. **90**, 063507 (2007).
- S. H. Jin, J. W. Kim, C. A. Lee, B.-G. Park and J. D. Lee, J. Korean Phys. Soc. **44**, 185 (2004).
- S. Pyo, M. Lee, J. Jeon, J. H. Lee, M. H. Yi and J. S. Kim, Adv. Funct. Mater. **4**, 619 (2005).
- S. Jeong, S. Lee, D. Kim, H. Shin and J. Moon, J. Phys. Chem. C **111**, 16083 (2007).
- K. H. Hass, Adv. Eng. Mater. **2**, 571 (2000).
- D. Lin-Vien, N. B. Colthup, W. G. Fateley and J. G. Grasselli, *The Handbook of Infrared and Raman Characteristic Frequencies of Organic Molecules* (Academic, Boston, 1991).
- C. J. Brinker and G. W. Scherer, *Sol-Gel Science* (Academic Press, San Diego, 1990).
- M. P. Stevens, *Polymer Chemistry* (Addison-Wesley, London, 1975).
- S. Jeong, D. Kim, S. Lee, B. K. Park and J. Moon, Appl. Phys. Lett. **89**, 092101 (2006).